

# Evaluating the Tree Population Density and Its Impacts in CLM-DGVM

SONG Xiang<sup>1,2</sup> (宋翔), ZENG Xiaodong<sup>\*1</sup> (曾晓东), and ZHU Jiawen<sup>1,2</sup> (朱家文)

<sup>1</sup>*International Center for Climate and Environment Sciences, Institute of Atmospheric Physics,*

*Chinese Academy of Sciences, Beijing 100029*

<sup>2</sup>*University of Chinese Academy of Sciences, Beijing 100049*

(Received 22 December 2011; revised 26 April 2012)

## ABSTRACT

Vegetation population dynamics play an essential role in shaping the structure and function of terrestrial ecosystems. However, large uncertainties remain in the parameterizations of population dynamics in current Dynamic Global Vegetation Models (DGVMs). In this study, the global distribution and probability density functions of tree population densities in the revised Community Land Model-Dynamic Global Vegetation Model (CLM-DGVM) were evaluated, and the impacts of population densities on ecosystem characteristics were investigated. The results showed that the model predicted unrealistically high population density with small individual size of tree PFTs (Plant Functional Types) in boreal forests, as well as peripheral areas of tropical and temperate forests. Such biases then led to the underestimation of forest carbon storage and incorrect carbon allocation among plant leaves, stems and root pools, and hence predicted shorter time scales for the building/recovering of mature forests. These results imply that further improvements in the parameterizations of population dynamics in the model are needed in order for the model to correctly represent the response of ecosystems to climate change.

**Key words:** Dynamic Global Vegetation Model, population dynamics, plant functional type, forest carbon storage, individual carbon allocation, carbon accumulation timescale

**Citation:** Song, X., X. D. Zeng, and J. W. Zhu, 2013: Evaluating the tree population density and its impacts in CLM-DGVM. *Adv. Atmos. Sci.*, **30**(1), 116–124, doi: 10.1007/s00376-012-1271-0.

## 1. Introduction

It is well known that the predominant characteristic of Dynamic Global Vegetation Models (DGVMs) is to simulate the distribution and structure of natural vegetation dynamically (Friend et al., 1997; Foley et al., 1998; Daly et al., 2000; Cox, 2001; Sitch et al., 2003; Levis et al., 2004; Woodward and Lomas, 2004), and this trait is described and controlled by various rules of vegetation dynamics. Generally speaking, vegetation dynamics may refer to two aspects: namely, population dynamics and individual dynamics. The former is usually described by establishment, mortality and competition among different species or plant functional types (PFTs) and determines the number of individuals as well as community structure, while the latter is related to phenology, carbon allocation

among the leaf, stem and root, as well as turnover.

Up to now, efforts to improve DGVMs have focused on the parameterizations of individual growth. There are various schemes allocating annual net primary production (NPP) to the individual leaf pool, stem pool and root pool proportionately (Friend et al., 1997; Levis et al., 2004; Ise et al., 2010), and the concept of dynamic allocation has gradually been adopted for further improvements (Friedlingstein et al., 1999; Oleson et al., 2010). Furthermore, the phenology schemes in most DGVMs usually relate carbon allocation and leaf green up/senescence to climate conditions, such as annual growing-degree days, temperature, soil moisture, and so on (Foley et al., 1998; Sitch et al., 2003; Levis et al., 2004; Arora and Boer, 2005; Oleson et al., 2010).

However, not much work has focused on population

---

\*Corresponding author: ZENG Xiaodong, xdzeng@mail.iap.ac.cn

dynamics, and its details differ among current models. Initially, forest gap models described forest dynamics based on individual establishment, growth and mortality of species on a gap-sized patch of land, typically less than 0.1 ha (Bugmann, 1996, 2001; Price et al., 2001). Although this method is effective to simulate forest structure and building processes, the parameterizations need large quantities of observational data, and the simulation of ecological processes in one gap needs to run hundreds of the stochastic processes with forest gap models, which causes a very large amount of calculation if the same parameterization is used for global simulation. Therefore, in order to represent the large scale vegetation dynamics in a computationally efficient way, many DGVMs describe the dynamics of different PFT populations instead of explicitly considering the interactions between plant individuals (Prentice et al., 2007). As we know, population dynamics not only has a close relationship with community structure and succession, but also has remarkable effects on individual growth. For example, individuals growing in regions with high competition (e.g. dense vegetation canopy) usually allocate more of their net primary production (NPP) to the stem in order to grow taller and outcompete others for light, and/or to the root to acquire belowground resources. Meanwhile, the average individual biomass in such environments may also be less than in regions with favorable conditions. Unfortunately, due to a lack of large-scale observational data and the complexity of processes, the parameterization schemes of population dynamics, e.g. establishment and mortality, feature many uncertainties (Bugmann, 2001), especially in DGVMs where the corresponding ecological processes are highly simplified.

In the work reported in this paper, the revised Community Land Model-Dynamic Global Vegetation Model (CLM-DGVM) was used as a test-bed to evaluate the distribution of population density and its effects on ecosystem characteristics (carbon storage, allocation, accumulation time scale).

## 2. The model

A DGVM (Levis et al., 2004) coupled with the Community Land Model (Oleson et al., 2004) (default CLM3.0-DGVM) was developed to simulate the global distribution of natural vegetation. It considers the processes of photosynthesis, respiration, phenology, carbon allocation, competition, survival and establishment, mortality, litter decomposition, soil respiration and fire disturbance. The details of the model were described by Levis et al. (2004). A revised CLM3.0-DGVM (Zeng et al., 2008; Zeng, 2010) introduced a

sub-module of temperate and boreal shrubs, incorporated with the “two-leaf” scheme for photosynthesis, as well as a new definition of fractional coverage ( $F$ ; %) for woody PFTs, i.e.

$$F = \sigma \cdot P, \quad (1)$$

instead of

$$F = \sigma \cdot P \cdot F_{\text{ind}}, \quad (2)$$

where  $\sigma$  ( $\text{m}^2$ ) is the average individual’s crown area;  $P$  (individuals  $\text{m}^{-2}$ ) is the population density (number of individuals per naturally vegetated area);  $F_{\text{ind}}$  (%) is the individual fractional projective cover (i.e. the percentage of crown area covered by leaves) (Levis et al., 2004), which was removed for the consistent treatment of the calculation of photosynthesis, respiration, and leaf area index in the revised model (Zeng et al., 2008; see Appendix A).

The revised model includes seven tree (Table 1), two shrub and three grass PFTs. Tree and shrub PFTs are called woody PFTs, and their population densities are determined by establishment, competition, mortality and fire. Furthermore, vegetation dynamics are represented in terms of average individuals, i.e. there are no age structure or size classes, and the net primary production is equally divided among individuals belonging to the same PFT. On the other hand, the model does not calculate the population density for grass PFTs.

When driven by observed near-surface atmospheric forcing data, the default and revised CLM-DGVM can roughly reproduce the regimes of forest, grassland, shrubland, and desert, as well as the zonal distributions of these vegetation types. Furthermore, the dependences of vegetation distribution on climate conditions derived from the model are in good agreement with observation data (Bonan and Levis, 2006; Zeng, 2010). The performance of the model coupled with a GCM—the Community Atmosphere Model (CAM)—has also been evaluated (Bonan and Levis, 2006).

**Table 1.** Tree PFTs.

Abbreviation	Full name
NEM-Tr	Temperate needleleaf evergreen tree
NEB-Tr	Boreal needleleaf evergreen tree
BET-Tr	Tropical broadleaf evergreen tree
BEM-Tr	Temperate broadleaf evergreen tree
BDT-Tr	Tropical broadleaf deciduous tree
BDM-Tr	Temperate broadleaf deciduous tree
BDB-Tr	Boreal broadleaf deciduous tree

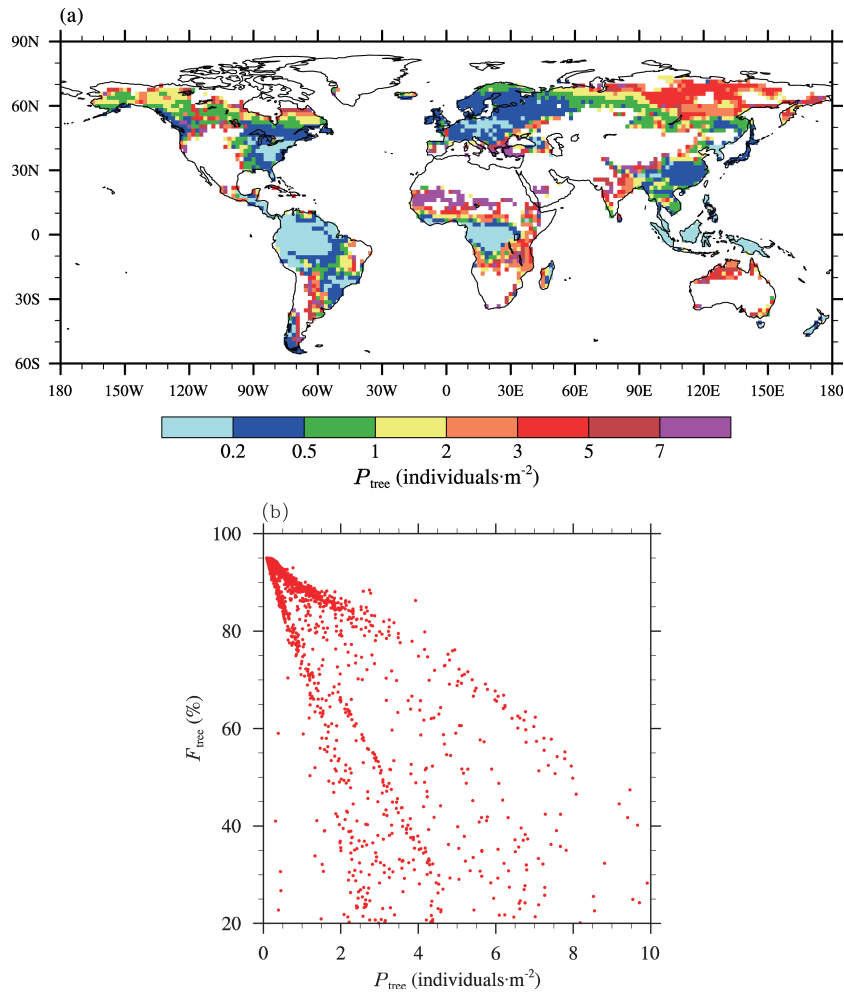


**Fig. 1.** (a) The simulated global distribution of total population density of tree PFTs ( $P_{tree}$ ; individuals  $m^{-2}$ ) (statistical condition:  $F_{tree} > 1\%$ ); (b) The relationship between total population density of tree PFTs ( $P_{tree}$ ; individuals  $m^{-2}$ ) and their total fractional coverage ( $F_{tree}$ ; %) simulated by the revised CLM-DGVM (statistical condition:  $F_{tree} \geq 20\%$ ).

### 3. Results

In order to evaluate the effects of population dynamics in the DGVM, a 600-year global offline simulation at T-62 resolution ( $192 \times 79$  grid cells covering  $60^\circ S - 90^\circ N$ ) was performed by running the revised CLM-DGVM, forced with 12 repetitions of 50 years of reanalysis surface atmospheric fields (1950–1999) from Qian et al. (2006). The first 550 years were used to spin-up for most grid cells finishing ecosystem succession and approaching the steady state, and the variables were averaged over the last 50 simulation years in the following statistics. For comparison, a similar simulation using the default CLM3.0-DGVM was also performed.

Because there is no global observational data of forest population density, data summarized from six Chinese forest observation stations were used for model

evaluation (see Table 2). These data were all collected from natural forests, covering tropical forests to temperate forests and montane coniferous forests.

#### 3.1 Simulated global distribution of tree population density and crown area

In the model, population density is also the most direct variable describing population dynamics, and tree PFTs have the highest competition priority, their global distribution directly determining the distribution and fractional coverage of other PFTs. Therefore, in this paper, only the population dynamics of tree PFTs are discussed.

Figure 1a shows the simulated global distribution of tree population density ( $P_{tree}$ ; individuals  $m^{-2}$ ) where tree coverage is larger than 1%. In the core area of tropical and temperate forests, e.g. the Amazon, Central Africa, Indonesia, eastern USA, Europe,

**Table 2.** Population density observational data from six forest observation stations in China.

Observation station	Location	Year	Stage of succession	Observation Area (m <sup>2</sup> )	Forest type	Population density (individuals m <sup>-2</sup> )
Xishuangbanna station in Yunnan	101°12'1"E, 21°57'40"N	2006	Natural mature forest (top of succession)	10 000	Tropical monsoon forest	0.289
	101°16'23"E, 21°55'08"N	2006	Natural secondary forest (middle-aged forest, middle and later period of building phase)	5000	Tropical monsoon forest	0.253
Ailao Shan station in Yunnan	101°16'59"E, 21°54'42"N	2006	Natural mature forest	2500	Tropical monsoon forest	0.318
	101°16'11"E, 21°55'16"N	2006	Natural secondary forest (young forest, early period of building phase)	2500	Tropical monsoon forest	0.236
Ji County station in Shaanxi	101°01'E, 24°32'N	2005	Natural mature forest	10 000	Sub-tropical mid-montane moist evergreen broad-leaved forest	0.126
	101°01'55"E, 24°32'10"N	2005	Natural mature forest	2500	Sub-tropical mid-montane moist evergreen broad-leaved forest	0.144
Qinling Mountains station in Shaanxi	110°43'46"E, 36°16'3"N	2006	Natural secondary forest (age of stand is 20 years)	1600	Warm-temperate deciduous broad-leaved forest	0.166
	108°26'51"E, 33°26'10"N	2008	Natural secondary forest (top of succession)	400	Temperate coniferous forest	1.275
Gongga Mountain station in Sichuan	108°26'24"E, 33°26'10"N	2008	Natural secondary forest	400	Temperate coniferous forest	0.253
	108°28'46"E, 33°27'17"N	2008	Natural secondary forest	400	Temperate coniferous forest	0.120
Linzhi station in Tibet	108°27'14"E, 33°25'58"N	2008	Natural secondary forest	400	Mixed temperate coniferous forest	0.128
	108°28'45"E, 33°27'15"N	2008	Natural secondary forest	400	Mixed temperate coniferous forest	0.257
Gongga Mountain station in Sichuan	101°59'19"E, 29°34'23"N	2005	Natural mature forest	2500	Subalpine dark coniferous forest	0.036
	101°59'54"E, 29°34'34"N	2005	Natural mature forest	1200	Mixed subalpine dark coniferous forest	0.177
Linzhi station in Tibet	94°42'45"E, 29°38'53"N	2006	Natural overmature forest (top of succession)	10 000	Montane coniferous forest	0.086

Note: The information in this table was collected from Cheng and Wang (2010), Deng and Tang (2010), Xu and Luo (2010), Zhang (2010), Zhang and Liu (2011) and Zhu et al. (2010).

and southeastern China, the tree population density was simulated as lower than  $0.5 \text{ individuals m}^{-2}$ , which is reasonable. However, in the peripheral areas of the core forests, as well as boreal forests,  $P_{\text{tree}}$  was much higher, especially in the north of Central Africa, where it was simulated to be greater than 7  $\text{individuals m}^{-2}$ . Unlike in forest gap models, CLM-DGVM does not allow the overlapping of vegetation canopies and, obviously, such a high population density is unreasonable, based on the observational data shown in Table 2.

Figure 1b shows the correlation between simulated tree population density and fractional coverage. In the areas with forest coverage greater than 90%, tree population densities ( $P_{\text{tree}}$ ) were always simulated to be less than 1  $\text{individual m}^{-2}$ . Forest coverage decreased as population density increased, but was still larger than 80% in some grid cells with  $P_{\text{tree}} \sim 2$ , and larger than 50% as  $P_{\text{tree}} \sim 8$ . Obviously, the role played by forests with a high tree population density cannot be ignored in the model. A direct evaluation of the simulated global distribution of tree population density is difficult because of the paucity of corresponding observational data and a lack of research on the impact of population density on vegetation–soil–atmosphere interactions. Therefore, instead, individual crown area ( $\sigma$ ) was chosen as an index of the ecosystem structure. As a mean-field model, individuals of the same PFT in CLM-DGVM have the same size of crown area, which reflects the balance between individual growth and population death. Figure 2 shows the correlation between simulated PFT population density and crown area for  $F_{\text{PFT}} \geq 20\%$ . Big trees (i.e. with a large  $\sigma$ ) only occurred if  $P$  was small, while areas with large  $P$  only yielded small trees. Figures 1b and 2 together imply that forests with lower tree coverage usually have a higher population density with smaller-sized trees. However, this is counter to what we know to be true from observing the natural world. Field observations by Harcombe (1987) revealed that individuals with a low growth rate usually have a much higher (stress-related) mortality rate. Therefore, an ecosystem with a large population of small trees could only be found in the early stage of succession, and not in mature forests.

To further investigate the formation of the simulated forests, the frequency distribution of crown area of trees was calculated, as shown in Fig. 3. In order to focus on the core area of forests, only the cases with the fractional coverage ( $F$ ) of a tree PFT greater than 50% was calculated (except for Fig. 3b). About 40% of the core forest area had trees with crown area below  $3 \text{ m}^2$ , and 18% below  $1 \text{ m}^2$  (Fig. 3a). Actually, for the whole forest area, the corresponding numbers

were even higher: 51% and 26% respectively (Fig. 3b). For comparison, Fig. 3c shows results from the default model and, as can be seen, they were similar to Fig. 3a, in so far as about 51% of the core forest area had trees with crown area below  $3 \text{ m}^2$ , and 13% below  $1 \text{ m}^2$ . These results imply that crown areas of tree PFTs are universally underestimated by the model. However, the situation for the seven tree PFTs was different. For NEB-Tr, BDB-Tr and BDT-Tr, crown areas of trees in most of the core area were less than  $3 \text{ m}^2$  (Figs. 3d and e; BDB-Tr is omitted). For BDM-Tr, BEM-Tr and NEM-Tr, their crown areas were relatively reasonable, with most of the core area covered by trees with crown area larger than  $3 \text{ m}^2$  (Fig. 3f; BEM-Tr and NEM-Tr are omitted). For BET-Tr, its crown area was mostly larger than  $5 \text{ m}^2$  (up to about 97%) (figure omitted). Therefore, the model biases of crown area mainly exist in the NEB-Tr, BDB-Tr and BDT-Tr PFTs.

### 3.2 Impacts of population density on ecosystem characteristics

To further investigate the effects of the overestimation of  $P$ , the relationship between simulated population density ( $P_{\text{PFT}}$ ;  $\text{individuals m}^{-2}$ ) and carbon content ( $C_{\text{PFT}}$ ;  $\text{g C m}^{-2}$ ) for each tree PFT with  $F_{\text{PFT}}$  not less than 20% is shown in Fig. 4a.  $C_{\text{PFT}}$  obviously decreased with increasing  $P_{\text{PFT}}$ , i.e. communities with a higher population density usually had lower carbon content. Figure 4b reflects the impact of population density on carbon allocation, i.e. a higher proportion of carbon was stored in leaves when  $P_{\text{PFT}}$  increased. Note that higher  $P_{\text{PFT}}$  mostly occurred in either peripheral tropical and temperate forests (undergoing water constraints) or boreal forests (undergoing cold constraints). Because leaves are the only producers in plants, while stems and roots are suppor-

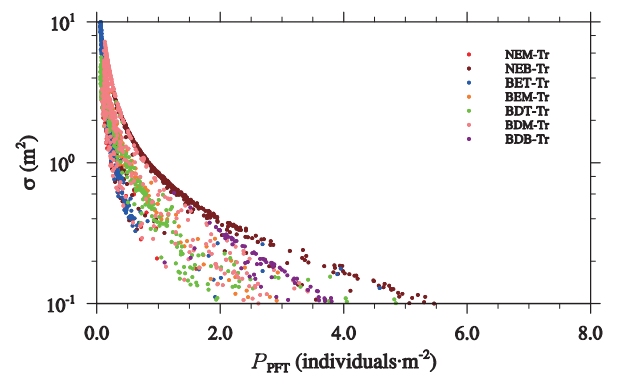


**Fig. 2.** The relationship between individual crown area ( $\sigma$ ;  $\text{m}^2$ ) and population density of the corresponding tree PFT ( $P_{\text{PFT}}$ ;  $\text{individuals m}^{-2}$ ) simulated by the revised CLM-DGVM (statistical condition:  $F_{\text{PFT}} \geq 20\%$ ).

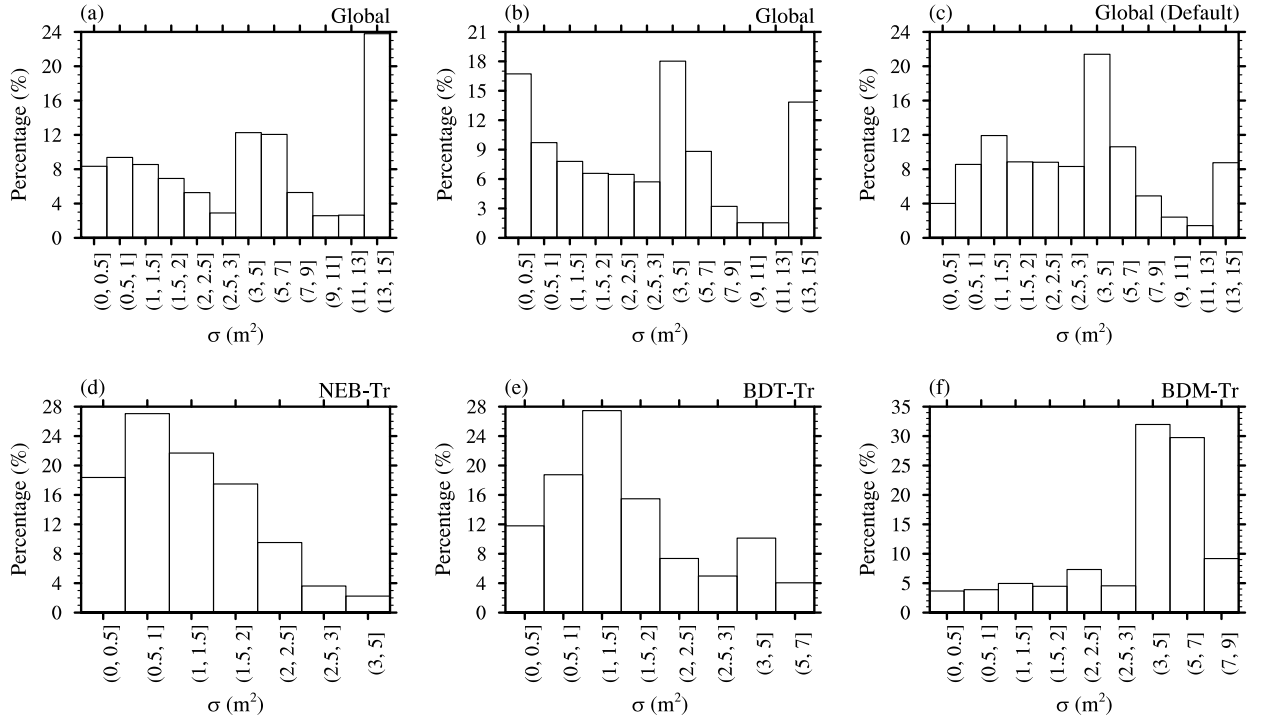


**Fig. 3.** (a)–(b) The frequencies of crown area ( $\sigma$ ;  $\text{m}^2$ ) of all the seven tree PFTs simulated by the revised CLM3.0-DGVM (statistical condition:  $F_{\text{PFT}} \geq 50\%$ ,  $F_{\text{PFT}} > 0$ , respectively); (c) The frequencies of crown area ( $\sigma$ ;  $\text{m}^2$ ) of all the seven tree PFTs simulated by the default CLM3.0-DGVM (statistical condition:  $F_{\text{PFT}} \geq 50\%$ ); (d)–(f) The frequency of crown area ( $\sigma$ ;  $\text{m}^2$ ) of three different tree PFTs simulated by the revised CLM3.0-DGVM (statistical condition:  $F_{\text{PFT}} \geq 50\%$ ).

tive organs (and hence carbon consumers), the higher  $C_{\text{leaf}}$  (leaf carbon per individual) to  $C_{\text{ind}}$  (the sum of leaf carbon, root carbon, sapwood carbon, as well as heartwood carbon per individual) ratio implies that the model may overestimate the individual productivity over these regions, leading to a greater forest coverage than expected.

These two features have great impacts on the simulation of ecosystem dynamics in response to climate variability and climate change. Under the same climate conditions, the too low carbon storage and relatively higher allocation rate to leaves in the ecosystem with higher population density imply that such an ecosystem may need a shorter time to build/recover. Similar to the definition of the biomass accumulation ratio in Ricklefs (2008), the timescale of carbon accumulation in the present work is defined as

$$T_{\text{PFT}} = \frac{C_{\text{PFT}}}{N_{\text{PFT}}}, \quad (3)$$

where  $T_{\text{PFT}}$  (years) is the timescale of carbon accumulation;  $C_{\text{PFT}}$  ( $\text{g C m}^{-2}$ ) is the total carbon content per unit area ( $\text{m}^2$ ) for each tree PFT; and  $N_{\text{PFT}}$  ( $\text{g C m}^{-2} \text{ yr}^{-1}$ ) is the annual net primary production per  $\text{m}^2$  for the corresponding tree PFT. Figure 4c

shows that, for tree PFTs, the timescale of carbon accumulation decreased when their population densities ( $P_{\text{PFT}}$ ; individuals  $\text{m}^{-2}$ ) increased, i.e. it may require a much shorter time to build/recover a forested ecosystem with higher  $P_{\text{PFT}}$ .

#### 4. Discussion

In this paper, the distribution of tree population density, as well as its impacts on ecosystem characteristics (such as carbon storage, allocation, and accumulation timescale) simulated by CLM-DGVM was evaluated. It was found that the model overestimated tree population densities, especially in boreal forests, but also in the peripheral areas of tropical and temperate forests. Meanwhile, individual crown areas of tree PFTs were underestimated by the model over these regions. The unrealistic high population density led to the underestimation of ecosystem carbon storage and the overestimation of carbon allocation to leaves, resulting in a relatively shorter timescale for the building or recovering of mature forests. These results imply that, although the model can roughly reproduce the global distribution of PFTs' fractional coverage, as well as the vegetation–climate relationships, it is incapable of capturing the timescale of ecosystem re-

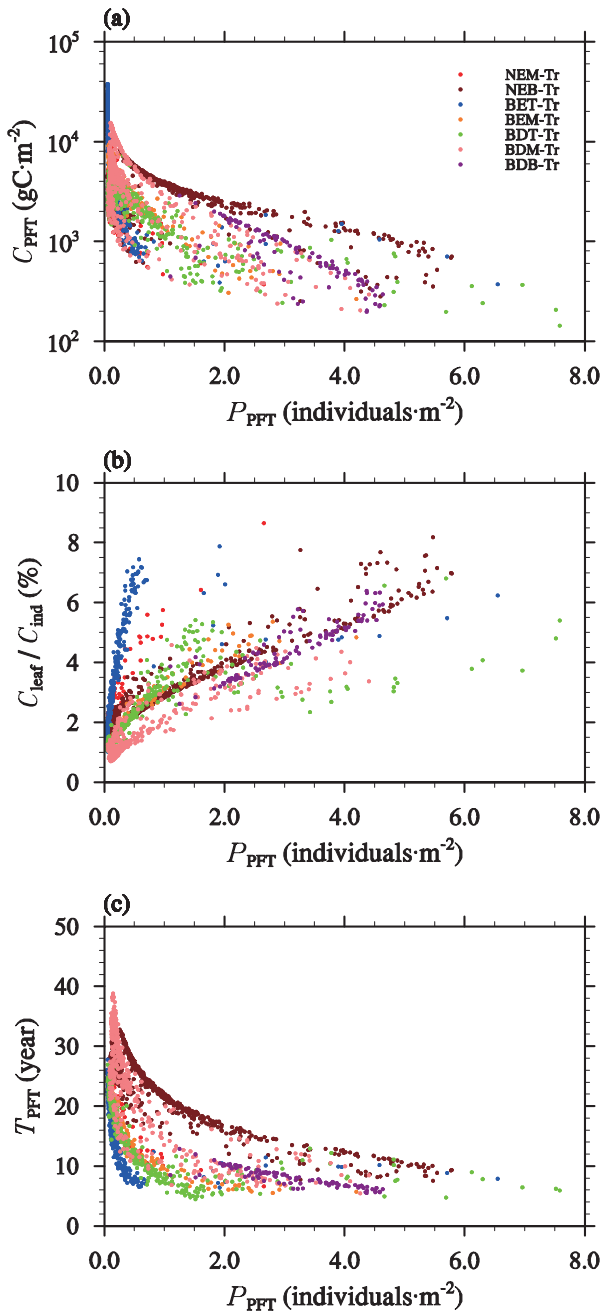


**Fig. 4.** (a) The relationship between simulated carbon content per unit area ( $C_{PFT}$ ;  $\text{g C m}^{-2}$ ) and population density ( $P_{PFT}$ ;  $\text{individuals m}^{-2}$ ) of each tree PFT (statistical condition:  $F_{PFT} \geq 20\%$ ); (b) The relationship between the ratio of the leaf carbon to the individual carbon ( $C_{\text{leaf}}/C_{\text{ind}}$ ; %) and each tree PFT's population density in vegetated area ( $P_{PFT}$ ;  $\text{individuals m}^{-2}$ ) simulated by the revised CLM-DGVM (statistical condition:  $F_{PFT} \geq 20\%$  and  $F_{\text{tree}} < 95\%$ ); (c) The relationship between population density ( $P_{PFT}$ ;  $\text{individuals m}^{-2}$ ) and the time scale of carbon accumulation ( $T_{PFT}$ ; year) simulated by the revised CLM-DGVM (statistical condition:  $F_{PFT} \geq 20\%$ ).

sponse to climate change, especially in those regions where the distribution of trees is subject to climate constraints.

The high population density results returned by the model could be caused by several reasons. First, the parameters used in the allometric functions relating vegetation height and crown area to stem diameter [Eqs. (24) and (25) of Levis et al., 2004] work well with tall trees, but lead to unrealistic small stem diameters and crown areas for relatively shorter vegetation. For example, for a tree that is 8 m high, its crown area is less than  $0.6 \text{ m}^2$  and stem diameter is as small as 4 cm. In the boreal region, or the dry tropical and temperate regions, where tree growth is slow due to climate constraints, the model tends to simulate the growth of such unrealistically small trees, and hence allows the coexistence of a large population. Second, the establishment scheme in the model only considers the shading effect of pre-existing trees on reducing the total establishment [Eq. (53) of Levis et al., 2004; see also Sitch et al., 2003]; it ignores the impacts of climate on seed germination rate and sapling survival rate. Hence, in areas with lower to medium tree coverage, the annual increment of tree population size due to establishment is overestimated by the model, resulting in high population densities so that the population decrement due to mortality can be balanced with establishment.

Such biases may account for the incorrect probability density functions (PDFs) of forest coverage in the model. In other work by our group (unpublished data), we have found that the model overestimates the percentage of forest core areas ( $F_{\text{tree}} > 70\%$ ) and underestimates the percentage of peripheral areas ( $F_{\text{tree}} < 40\%$ ). The results in the current paper imply that, if the biases of the high population density in the model were to be resolved, the relatively low productivities in the corresponding areas may lead to a decrease in forest coverage due to the increment of individual carbon storage and the decrement in carbon allocation to leaves. Hence, the proportion of regions with lower forest coverage will increase, especially for the NEB-Tr, BDB-Tr and BDT-Tr PFTs, and then the biases in PDFs of forest coverage in the model will be reduced.

Although our results were based on a revised CLM-DGVM, they should also be applied to other DGVMs with similar vegetation population dynamics, e.g. the original CLM3.0-DGVM, LPJ-DGVM, and CLM4-CNDV. Essential improvements in the parameterizations of the population dynamics schemes in DGVMs are required in order to capture future ecosystem changes in response to climate change.

**Acknowledgements.** This work was supported by

the Chinese Academy of Sciences (Strategic Priority Research Program; Grant No. XDA05110103) and the State Key Project for Basic Research Program of China (also called 973 Program, Grant No. 2010CB951801). The authors are grateful to the two anonymous reviewers and editors for their helpful comments and suggestions.

## APPENDIX A

### Modification of the Definition of Woody PFTs' Fractional Coverage

In CLM-DGVM,  $F$  is calculated by Eq. (2) and denoted as the fractional foliar projective cover [see Eq. (28) of Levis et al. (2004)], where

$$F_{\text{ind}} = 1 - e^{-0.5L_{\text{ind}}}$$

and  $L_{\text{ind}}$  is the total leaf area of an individual tree divided by its  $\sigma$  [Eqs. (26) and (27) of Levis et al., 2004]. The term  $F_{\text{ind}}$  implies that the fraction of bare soil within the  $\sigma$  is excluded.

However, such treatment is inconsistent with the calculation of photosynthesis, transpiration, and NPP. In the model, photosynthesis and evapotranspiration of a PFT are calculated using  $L_{\text{ind}}$ , i.e. they are averaged over  $\sigma$ . It is incorrect to use  $F$  as the weights in the calculation of grid-averaged photosynthesis and transpiration from the PFT ones. On the other hand, plant respiration is calculated as total PFT respiration divided by  $F$  [Eqs. (4)–(6) of Levis et al., 2004]. Hence, NPP cannot be calculated as the difference between photosynthesis and respiration [as in Eqs. (8) and (9) of Levis et al., 2004] because these fluxes are averaged over different areas.

## REFERENCES

- Arora, V. K., and G. J. Boer, 2005: A parameterization of leaf phenology for the terrestrial ecosystem component of climate models. *Global Change Biology*, **11**, 39–59.
- Bonan, G. B., and S. Levis, 2006: Evaluating aspects of the Community Land and Atmosphere Models (CLM3 and CAM3) using a dynamic global vegetation model. *J. Climate*, **19**, 2290–2301.
- Bugmann, H. K. M., 1996: A simplified forest model to study species composition along climate gradients. *Ecology*, **77**(7), 2055–2074.
- Bugmann, H. K. M., 2001: A review of forest gap models. *Climatic Change*, **51**, 259–305.
- Cheng, G. W., and G. X. Wang, 2010: Gongga Mountain station in Sichuan. *Forest Ecosystem*, Vol. 3, *Station Observation and Research Database of Chinese Ecosystem*, China Agricultural Press, Beijing, 150pp. (in Chinese)
- Cox, P. M., 2001: Description of the TRIFFID Dynamic Global Vegetation Model. Hadley Centre Tech. Note 24, Hadley Centre, Bracknell, U.K., 16pp.
- Daly, C., D. Bachelet, J. M. Lenihan, R. P. Neilson, W. Parton, and D. Ojima, 2000: Dynamic simulation of tree–grass interactions for global change studies. *Ecological Applications*, **10**(2), 449–469.
- Deng, X. B., and J. W. Tang, 2010: Xishuangbanna station in Yunnan. *Forest Ecosystem*, Vol. 3, *Station Observation and Research Database of Chinese Ecosystem*, China Agricultural Press, Beijing, 380pp. (in Chinese)
- Foley, J. A., S. Levis, I. C. Prentice, D. Pollard, and S. L. Thompson, 1998: Coupling dynamic models of climate and vegetation. *Global Change Biology*, **4**, 561–579.
- Friedlingstein, P., G. Joel, C. B. Field, and I. Y. Fung, 1999: Toward an allocation scheme for global terrestrial carbon models. *Global Change Biology*, **5**, 755–770.
- Friend, A. D., A. K. Stevens, R. G. Knox, and M. G. R. Cannell, 1997: A process-based, terrestrial biosphere model of ecosystem dynamics (Hybrid v3.0). *Ecological Modelling*, **95**, 249–287.
- Harcombe, P. A., 1987: Tree life tables. *Bioscience*, **37**, 557–568.
- Ise, T., C. M. Litton, C. P. Giardina, and A. Ito, 2010: Comparison of modeling approaches for carbon partitioning: Impact on estimates of global net primary production and equilibrium biomass of woody vegetation from MODIS GPP. *J. Geophys. Res.*, **115**, G04025, doi: 10.1029/2010JG001326.
- Levis, S., G. B. Bonan, M. Vertenstein, and K. W. Oleson, 2004: The Community Land Model's Dynamic Global Vegetation Model (CLM-DGVM): Technical description and user's guide. NCAR Technical Note, NCAR/TN-459+IA, National Center for Atmospheric Research, Boulder, NCAR, Colorado, 50pp.
- Oleson, K. W., and Coauthors, 2004: Technical Description of the Community Land Model (CLM). NCAR Technical Note, NCAR/TN-461+STR, National Center for Atmospheric Research, Boulder, Colorado, 174pp.
- Oleson, K. W., and Coauthors, 2010: Technical Description of version 4.0 of the Community Land Model (CLM). NCAR Technical Note, NCAR/TN-478+STR, National Center for Atmospheric Research, Boulder, Colorado, 257pp.
- Prentice, I. C., and Coauthors, 2007: Dynamic global vegetation modelling: Quantifying terrestrial ecosystem responses to large-scale environmental change. *Terrestrial Ecosystems in a Changing World*, Canadell et al., Eds., Springer-Verlag, Berlin, 175–192.
- Price, D. T., and Coauthors, 2001: Regeneration in gap models: Priority issues for studying forest responses to climate change. *Climatic Change*, **51**, 475–508.
- Qian, T. T., A. G. Dai, K. E. Trenberth, and K. W. Oleson, 2006: Simulation of global land surface condi-



- tions from 1948 to 2004. Part I: Forcing data and evaluations. *Journal of Hydrometeorology*, **7**, 953–975.
- Ricklefs, R. E., 2008: *The Economy of Nature*. 6th ed. W. H. Freeman and Company, 41 Madison Avenue, New York, 700pp.
- Sitch, S., and Coauthors, 2003: Evaluation of ecosystem dynamics, plant geography and terrestrial carbon cycling in the LPJ dynamic global vegetation model. *Global Change Biology*, **9**, 161–185.
- Woodward, F. I., and M. R. Lomas, 2004: Vegetation dynamics-simulating responses to climatic change. *Biological Reviews*, **79**, 643–670.
- Xu, A. S., and D. Q. Luo, 2010: Linzhi station in Tibet. *Forest Ecosystem*, Vol. 3, *Station Observation and Research Database of Chinese Ecosystem*, China Agricultural Press, Beijing, 108pp. (in Chinese)
- Zeng, X. D., 2010: Evaluating the dependence of vegetation on climate in an improved Dynamic Global Vegetation Model (CLM3.0-DGVM). *Adv. Atmos. Sci.*, **27**, 977–991, doi: 10.1007/s00376-009-9186-0.
- Zeng, X. D., X. B. Zeng, and M. Barlage, 2008: Growing temperate shrubs over arid and semiarid regions in the Community Land Model-Dynamic Global Vegetation Model. *Global Biogeochemical Cycles*, **22**, GB3003, doi: 10.1029/2007GB003014.
- Zhang, S. X., 2010: Qinling Mountains station in Shanxi. *Forest Ecosystem*, Vol. 3, *Station Observation and Research Database of Chinese Ecosystem*, China Agricultural Press, Beijing, 182pp. (in Chinese)
- Zhang, Y. P., and Y. H. Liu, 2011: Ailao Shan station in Yunnan. *Forest Ecosystem*, Vol. 3, *Station Observation and Research Database of Chinese Ecosystem*, China Agricultural Press, Beijing, 184pp. (in Chinese)
- Zhu, J. Z., Q. K. Zhu, J. G. Zhang, H. X. Bi, T. X. Wei, and X. P. Zhang, 2010: Ji County station in Shanxi. *Forest Ecosystem*, Vol. 3, *Station Observation and Research Database of Chinese Ecosystem*, China Agricultural Press, Beijing, 269pp. (in Chinese)